

## Improved Ultra-Wideband Rectennas Using Hybrid Resistance Compression Technique

Chaoyun Song, *Student Member, IEEE*, Yi Huang, *Senior Member, IEEE*, Jiafeng Zhou and Paul Carter

**Abstract**— This communication presents a novel hybrid resistance compression technique (HRCT) to improve the performance of broadband rectennas. The HRCT can offer resistance compression characteristic by reducing the nonlinear effects of the rectifier and provide improved impedance matching performance over a wide frequency range. Two ultra-wideband rectennas (with/without using the HRCT) have been designed, made and tested. The proposed rectennas have a very wide bandwidth from 450 to 900 MHz (covers the entire DTV, LTE700 and GSM900 bands in the UK) with relatively high conversion efficiency (up to 77%). The HRCT can maintain the high efficiency of the rectenna in a wide load impedance range (from 5 to 80 k $\Omega$ ). The measured harvested DC power of the rectenna from an outdoor ambient environment is about 66.7  $\mu$ W with an overall conversion efficiency of 42.2% which is therefore suitable for wireless energy harvesting to power low power electronic devices with different load impedance.

**Index Terms**—Broadband rectenna, rectifier, resistance compression, wireless energy harvesting.

### I. INTRODUCTION

AMBIENT wireless energy harvesting using broadband and multiband rectennas has emerged in recent years and attracted a lot of interest due to its advantages of accumulating more energy from the weak ambient power sources and producing a higher output power than that from a narrow band rectenna [1]. Harvesting energy from different channels and different sources simultaneously can significantly reduce the effect on the overall conversion efficiency of the rectenna (which is very significant at ambient low power levels) due to the intrinsic power consumption of devices [2]. However, the design of broadband and multiband rectennas is normally very challenging due to the strong nonlinearity of the rectifier. So far, there are very few multiband or broadband rectennas reported with a relatively good performance [3]–[8]. The performance of broadband rectennas can be easily affected by the variation in such as the input power level and load impedance.

A *resistance compression network* (RCN) is a special network that can reduce the sensitivity and nonlinearity of electronic devices such as amplifiers, DC-DC converters and rectifiers [9]–[13]. The large variation of load impedance can be compressed using this technique which results in the smaller variation of the input impedance of the circuit. Thus, the RCN

has been used in rectenna design to reduce the nonlinear effects when the loading condition is varying [9]. But, the performance of RCN heavily relies on the operating frequency of the network. The resistance compression characteristics are normally realized at limited operating frequencies. Consequently, most reported RCNs are single band RCNs [9], [11], and only one reported design is a dual-band RCN [13] but the available frequency bandwidth is narrow.

In this Communication, we propose a novel hybrid resistance compression technique (HRCT) that is aimed to improve the performance of broadband rectennas. A broadband impedance network is first proposed and introduced in Section II where the rectenna in this network has a very wide bandwidth from 450 to 900 MHz with relatively high conversion efficiency (up to 77%). Then, the broadband impedance matching network is mixed with a RCN to form an HRCT. The HRCT can offer resistance compression as well as improved impedance matching performance over the frequency band of interest. The theory and rectenna design example using the proposed HRCT are discussed in Section III. The improved rectenna (using the HRCT) is still of a broad bandwidth (470 to 880 MHz) and high efficiency. An important feature is that the conversion efficiency of the improved rectenna is more stable than that of the original rectenna when the load impedance varies in a wide range (from 5 to 80 k $\Omega$ ). Section IV introduces the measured performance of both rectennas in an outdoor ambient environment, where an output harvested power of 66.7  $\mu$ W was measured. The improved rectenna has a more consistent performance than the original one in terms of overall conversion efficiency. Finally, conclusions are drawn in Section V. To the best of our knowledge, it is the first time to apply the resistance compression technique in broadband rectenna designs.

### II. ULTRA-WIDEBAND RECTIFIER DESIGN

The design of impedance matching network for broadband rectennas is very challenging since the input impedance of the rectifier varies significantly as a function of frequency, input power and load impedance [14]. It is required to optimize the matching network under the aforementioned conditions. As a consequence, the broadband rectennas in [3]–[5] introduced a complicated design procedure and therefore reported complex matching networks. In this work, we aim to design a simple broadband matching network using a new method. The proposed matching network can achieve good performance over a wide frequency band, input power level and load impedance range.

As a starting point of the design, a simple yet efficient matching network is proposed for ultra-wideband rectennas (with a fractional bandwidth > 30%). The network is based on a shunt and series LC bandpass matching topology, as shown in Fig. 1(a). This matching topology can work well over a given frequency band (between  $f_0$  and  $f_i$ ) by selecting appropriate values for the lumped elements (e.g., inductors and capacitors) [13]. Secondly, a modified L-network is added to the LC bandpass matching topology to enhance the performance as shown in Fig. 1(b), which is similar to [4]. The operating

Manuscript received August 11, 2016; revised December 3, 2016; accepted January 1, 2017. This work was supported in part by the Engineering and Physical Sciences Research Council, U.K., and in part by the Aeternum LLC. (Corresponding author: Yi Huang)

C. Song, Y. Huang, and J. Zhou are with the Department of Electrical Engineering and Electronics, University of Liverpool, Liverpool L69 3GJ, U.K. (e-mail: sgcsong2@liv.ac.uk; yi.huang@liv.ac.uk ;).

P. Carter is with Global Wireless Solutions, Inc., Dulles, VA 20166 USA

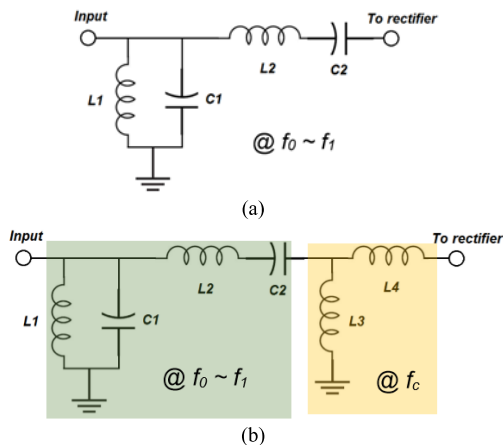


Fig. 1. Proposed impedance matching networks for broadband rectennas. (a) The LC bandpass matching topology. (b) The LC bandpass and modified L-network matching topology.

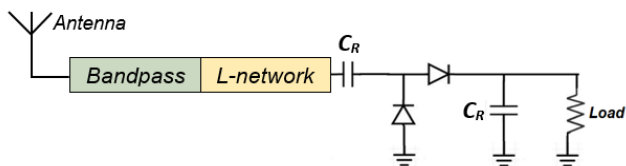


Fig. 2. Configuration of the proposed rectenna using the bandpass and L-network matching topology.

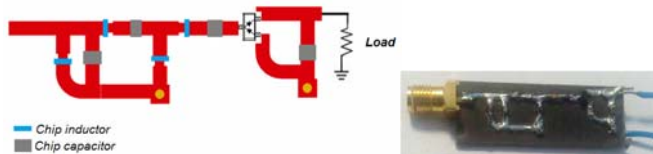


Fig. 3. Topology of the proposed ultra-wideband rectifier and the fabricated prototype. The size of the PCB is  $3.5 \times 1 \text{ cm}^2$ .

frequency of this L-network is set as the center frequency of the frequency band of interest, where  $f_c = (f_i + f_0)/2$ . The performance of the complete broadband matching network can be improved by optimizing the values of components according to the frequency band.

As an example, we have designed an ultra-wideband rectifier using the proposed matching network. The start frequency ( $f_0$ ) and stop frequency ( $f_i$ ) are selected as 450 MHz and 900 MHz respectively, thus the center frequency ( $f_c$ ) is 675 MHz and the fractional bandwidth (FBW) is about 67%. The reason for selecting this frequency band is that it covers the entire DTV bands in the U.K. (channels 21–68 from 470 to 850 MHz) as well as the mobile LTE700 and GSM900 bands. Therefore, the proposed rectenna would be very suitable for wireless energy harvesting from 48 DTV channels (8 MHz bandwidth of each) and two mobile bands (about 50 MHz bandwidth of each) simultaneously. The configuration of the proposed rectenna is shown in Fig. 2, where a standard 1-stage voltage doubler rectifier is selected due to its high conversion efficiency [14]. The rectifying diodes are SMS7630 from Skyworks. The ADS software is employed to design and optimize the rectifier. The Large Signal S-parameter (LSSP) simulation and Harmonic

TABLE I  
CIRCUIT COMPONENTS USED IN THE DESIGN

Component name	Nominal Value	Part number and supplier
L1	6.8 nH chip inductor	0603HP6N8, Coilcraft
C1	3.8 pF chip capacitor	GRM1885C1H3R8, Murata
L2	1.8 nH chip inductor	0603HP1N8, Coilcraft
C2	2.5 pF chip capacitor	GRM1885C1H2R5, Murata
L3	22 nH chip inductor	0603HP22N, Coilcraft
L4	68 nH chip inductor	0603HP68N, Coilcraft
C <sub>R</sub>	100 nF chip capacitor	GRM188R71H104, Murata

Balance (HB) simulation are used to optimize the values of the components (as shown in Fig.1 (b)). In addition to the operating frequency, the effects of the input power to the diode impedance should also be taken into account. The input power of the rectifier is optimized for a range of input power levels from -30 to 0 dBm (to match with the typical ambient signal levels). Note that here the rectifier is only optimized for a wide frequency band and input power range, since the rectifier performance vs. load can be enhanced by using the resistance compression technique (which will be discussed in the following sections). Thus a typical load resistor of 5 k $\Omega$  is selected in the simulation. After the rectifier has been optimized, the ideal lumped-element is replaced by using real product models provided by the suppliers (such as Coilcraft and Murata). An accurate EM tuning is conducted to improve the accuracy of the results. The final values and part numbers of the chip inductors and capacitors are given in Table I. The topology of the proposed rectifier is shown in Fig. 3. A fabricated example is shown as well. The substrate is Rogers Duriod5880 with a relative permittivity of 2.2 and a thickness of 1.575 mm.

The simulated and measured reflection coefficients  $S_{11}$  and RF-DC conversion efficiency of the rectifier are shown in Figs. 4(a) and (b) as a function of frequency for different input power levels. The conversion efficiency is obtained using

$$\eta_{RF-dc} = \frac{P_{DC}}{P_{in}} \quad (1)$$

where  $P_{DC}$  is the output DC power and  $P_{in}$  is the input RF power to the rectifier. It can be seen that the rectifier is of a very wide bandwidth (from 0.45 to 0.9 GHz) and works well at the desired input power levels. The conversion efficiency is high over the band of interest. The measured efficiency is a bit smaller (about 5%) than the simulated results. This is because that the loss of the components and diodes in reality is higher than the loss of the product models used in the simulation. The measured and simulated conversion efficiency versus the input power level at two frequencies are depicted in Fig. 5. It can be seen that the efficiency increases linearly with the input power (from -30 to 0 dBm). The peak efficiency (up to 77%) is achieved at -1 dBm input power, then the efficiency starts to decrease due to the breakdown of the diodes. The measured and simulated conversion efficiency at the desired frequencies are depicted in Fig. 6 for different load resistances. Since the load resistance in

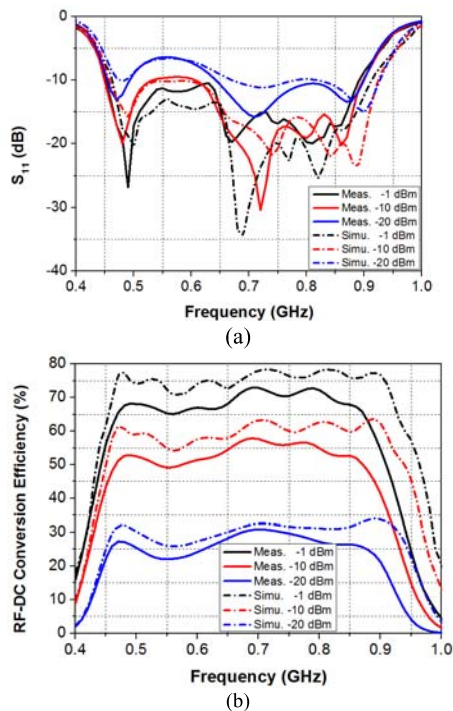


Fig. 4. The measured and simulated (a)  $S_{11}$  and (b) RF-DC conversion efficiency of the rectifier versus frequency at three different input power levels.

the optimization is 5 k $\Omega$ , it is found that the highest efficiency in all cases is achieved for the load impedance of around 5 k $\Omega$ . The efficiency decreases rapidly when the load impedance is larger than 5 k $\Omega$ . This is due to the impedance mismatch caused by the nonlinear effects of the rectifier. It is required to solve this problem for wireless energy harvesting in many applications [15].

### III. HYBRID RESISTANCE COMPRESSION TECHNIQUE

To overcome the aforementioned drawback and reduce the nonlinear effects of the ultra-wideband rectifier, a novel hybrid resistance compression technique (HRCT) is introduced in this Section. The fundamental circuit model of a typical RCN is shown in Fig. 7, where the network consists of two branches that exhibit opposite phase response of the input impedance at a given frequency. In this way, the input impedance of the network ( $Z_{in}$ ) could experience small variations when the load impedance ( $R_L$ ) varies significantly [9]. Such RCNs can be used to reduce the sensitivity of many nonlinear circuits, such as rectifiers, amplifiers and DC-DC converters [10]. However, since the performance of the RCN is heavily dependent on the operating frequency, the available frequency bandwidth of the RCN is normally very narrow (e.g. FBW < 10%). Most reported designs are therefore single band RCNs [9]–[11].

Here we propose an HRCT with the aim to extend the frequency bandwidth of RCNs. Based on the initial broadband matching network proposed in Section II, a secondary network is introduced. As shown in Fig. 8, the initial network is placed on the upper branch while the second network is configured on the lower branch. It is noted that the two networks use the identical circuit components, but a slightly transformed order for some of the components. From [13], the opposite phase response in such 4<sup>th</sup> order shunt and series LC networks (as

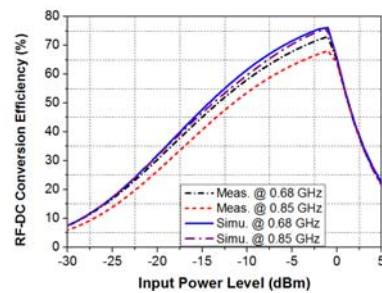


Fig. 5. The measured and simulated RF-DC conversion efficiency of the rectifier versus input power level at 0.68 GHz and 0.85 GHz.

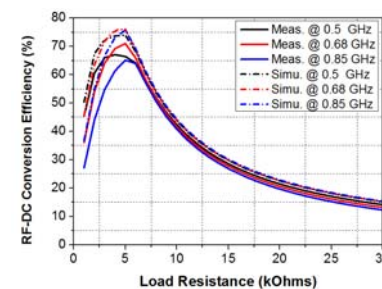


Fig. 6. The measured and simulated RF-DC conversion efficiency of the rectifier versus load resistance at three different frequencies. The input power level is -1 dBm.

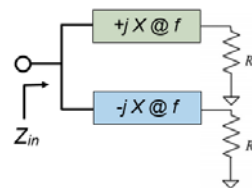


Fig. 7. Fundamental circuit model of a resistance compression network.

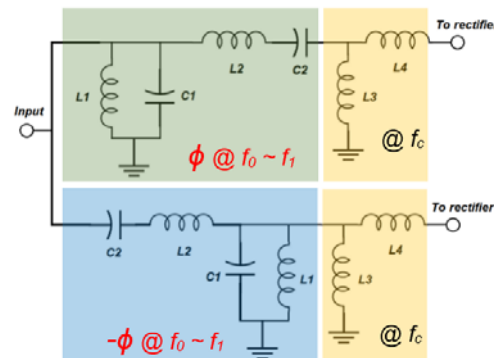


Fig. 8. The proposed matching network using the HRCT, the LC bandpass matching topology is converted on the second branch to achieve opposite phase response ( $\phi$  and  $-\phi$ ) of the input impedance.

shown in Fig. 1(a)) can be achieved by reversing their input and output ports. Thus, the shunt and series LC bandpass matching topology (in the initial network) is converted to a series and shunt CL bandpass matching topology (in the secondary network). The initial network shows a positive phase response ( $\phi$ ) of the input impedance over the covered frequency band (between  $f_0$  and  $f_1$ ), while the second network achieves opposite phase response ( $-\phi$ ) for the frequency band of interest. Meanwhile, the modified L-networks for impedance matching in both branches are maintained. Thus, the proposed matching



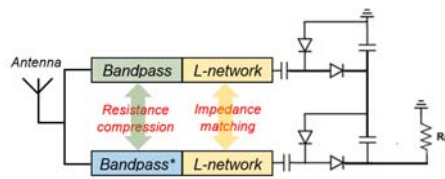


Fig. 9. Configuration of the improved broadband rectenna using the HRCT.

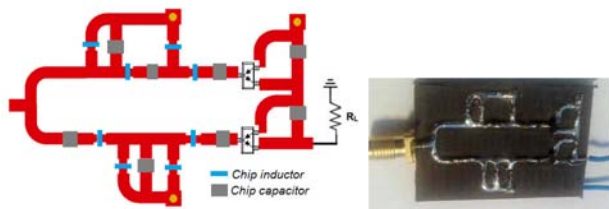
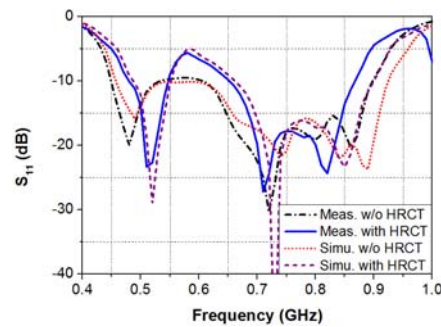


Fig. 10. Topology of the improved broadband rectenna using the HRCT and the fabricated prototype rectifier. The size of PCB is  $4.5 \times 2.5 \text{ cm}^2$ .

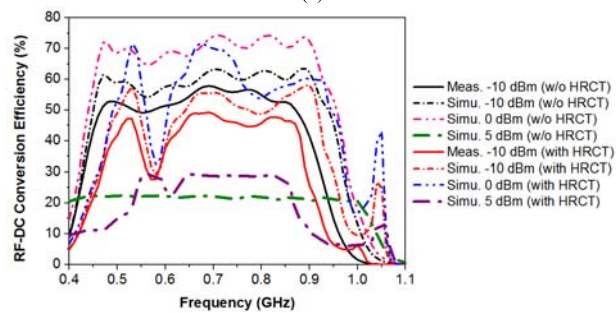
network may have resistance compression characteristics (opposite phase response of the input impedance) within the frequency band of interest, and have an enhanced impedance matching performance at the center frequency. The RCN is mixed with impedance matching network to form an HRCT.

The configuration of the proposed rectenna using the novel HRCT is shown in Fig. 9, where the circuit components and diodes are the same as shown in Section II and Table I. Two identical voltage doubler rectifiers are connected to the output ports of the network. The outputs of the rectifiers are connected in series in order to increase the output voltage [4]. The proposed HRCT can offer resistance compression as well as impedance matching performance. The topology and fabricated example of the improved broadband rectifier using such HRCT are shown in Fig. 10. The substrate is still Rogers Duriod5880. It is noted that the final circuit has an input power divider on the PCB. However, since the matching network is designed based on lumped-element network, the effect of the power divider on the input impedance of the rectifier is relatively small. Here the width of the microstrip lines is selected as 1.5 mm.

The measured and simulated  $S_{11}$  and RF-DC conversion efficiency of the rectifiers with and without using the HRCT are shown in Fig. 11 as a function of frequency. The input power is -10 dBm (total channel power of the outdoor DTV signal [16]). It can be seen that the improved rectifier (using the HRCT) is still of a broad bandwidth with relatively high conversion efficiency over the band of interest. The bandwidth of the improved rectifier is from 0.47 to 0.88 GHz, which is slightly narrower than the bandwidth of the initial rectifier (without using the HRCT). This is probably due to the parasitic behavior of the SMD components used in the circuit. In addition, the simulated conversion efficiency of both rectifiers for three different input power levels are shown in Fig. 11 as well. The efficiency is about 75% at 0 dBm but about 25% at 5 dBm. This is partially due to the breakdown of the diodes and partially due to the impedance mismatch at higher input powers. The measured and simulated conversion efficiency versus load resistance of the two rectifiers are shown in Fig. 12. The frequency is at the center frequency of the band (0.68 GHz). It can be seen that the improved rectifier has relatively consistent



(a)



(b)

Fig. 11. The measured and simulated (a)  $S_{11}$  and (b) RF-DC conversion efficiency of the rectifiers with/without using the HRCT versus frequency. The input power level is -10 dBm and load resistance is 5 k $\Omega$ . The simulated conversion efficiency for the input power level at 0 and 5 dBm is shown as well.

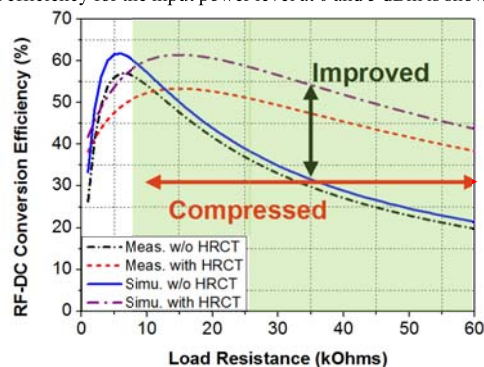


Fig. 12. The measured and simulated RF-DC conversion efficiency for the rectifiers with/without using the HRCT versus load resistance. The input power level is -10 dBm and the frequency is 0.68 GHz.

efficiency (over 40%) for the load resistance from 5 to 60 k $\Omega$ . The peak efficiency is about 60% for the load resistance of 15 k $\Omega$ . The efficiency roll-off of the initial rectifier (vs. load) has been significantly suppressed. The HRCT has indeed compressed the variation of the load resistance and reduced the non-linear effects of the rectifier. The contour plots of the simulated and measured conversion efficiency of the rectifier using the HRCT are shown in Figs. 13 (a) and (b). It can be seen that the improved rectifier has consistent efficiency (e.g. > 40%) over the frequency band of interest (0.5 – 0.9 GHz) and a wide load impedance range (5 – 50 k $\Omega$ ). It demonstrates that the proposed HRCT has indeed extended the frequency bandwidth of the RCN. The rectenna using the HRCT can be broadband and of high conversion efficiency over a wide load impedance range, which is highly significant for wireless energy harvesting in many real-world applications (different equivalent load values).

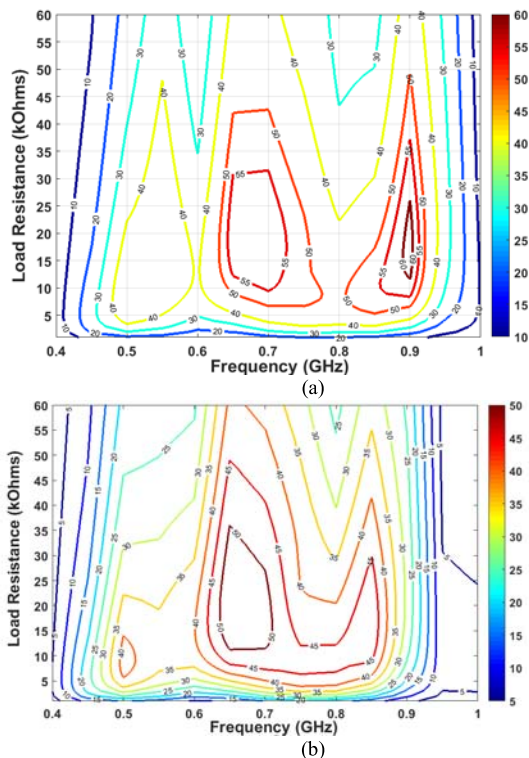


Fig. 13. The simulated (a) and measured (b) RF-DC conversion efficiency of the rectifier using the HRCT versus load resistance and frequency. The input power level is -10 dBm.

#### IV. RECTENNA MEASUREMENTS IN REALITY

The rectifier was connected to an ultra-wideband circular polarization (CP) receiving antenna (as proposed in [4]) to form a broadband rectenna. The receiving antenna has a very wide bandwidth (from 0.5 to 2.5 GHz) and an average gain of around 3.5 dBi over the frequency band. The performance of the rectenna was directly evaluated in reality, where an outdoor ambient environment in Liverpool, UK was selected. As shown in Fig. 14, the measurement location was in a relatively open environment without a cluster of tall buildings that may block the wireless signals. The received power by the antenna versus frequency was measured by using a portable spectrum analyzer and the results are shown in Fig. 15. It can be seen that the powers at DTV channels 21-31, 39-65, LTE700 and GSM900 bands were observed with an average power level of around -35 dBm over the frequency band. The average total channel power (DTV+LTE+GSM) was obtained using the same approach as proposed in [5], where a wideband power sensor was employed to record the power as a function of time. As a result, the average total channel power in this scenario was found to be around -8 dBm (158  $\mu$ W). The output DC voltage of the rectennas with/without using the HRCT was measured by using a voltage meter and the harvested DC power was obtained using  $P_{DC} = V^2/R_L$ , where  $R_L$  is the load resistance. As shown in Fig. 14, the measured output voltage of the rectenna using the HRCT was about 1 V (load resistance is 15 k $\Omega$  for the maximum conversion efficiency). Thus the harvested DC power was found to be 66.7  $\mu$ W. The overall conversion efficiency of the rectenna can be calculated using

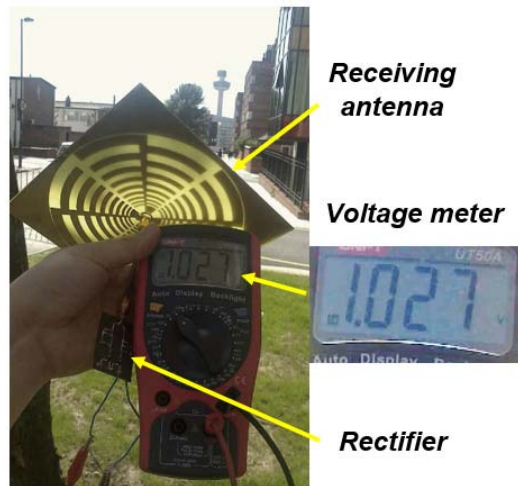


Fig. 14. The rectenna measurement in an outdoor ambient environment.

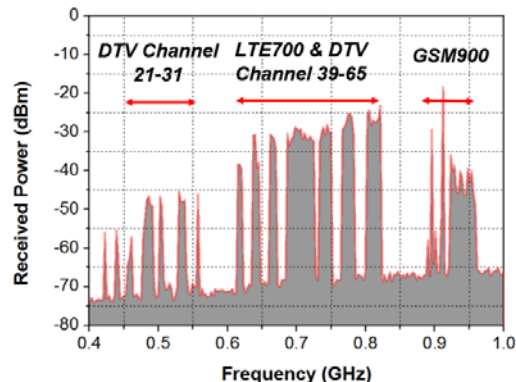


Fig. 15. The measured received power (in dBm) versus frequency of the broadband rectenna.

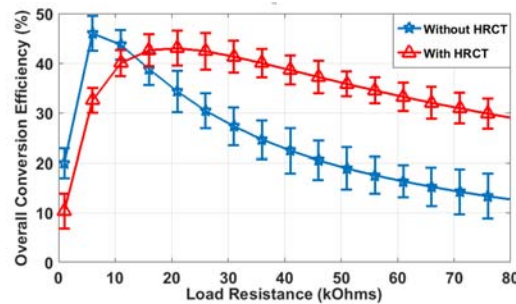


Fig. 16. The measured overall RF-DC conversion efficiency of the rectennas with/without using the HRCT. The results are shown with error bars.

$$\eta_{overall} = \frac{P_{DC}}{P_T} \quad (2)$$

where  $P_T$  is the total channel power (158  $\mu$ W). Thus in this scenario, the overall conversion efficiency was about 42.2%. Moreover, the rectennas with and without using the HRCT were measured by using different load resistances from 1 to 80 k $\Omega$ . The experiment was conducted in multiple times to improve the accuracy of results. The overall conversion efficiency is shown in Fig. 16 with error bars. It can be seen that the efficiency of the rectenna without using the HRCT reaches the peak value (50%) at 5 k $\Omega$  load resistance, and decreases rapidly for larger load resistance (from 15 to 80 k $\Omega$ ). The

TABLE II  
COMPARISON WITH OTHER RELATED DESIGNS

Ref. (year)	Frequency (GHz)	FBW (%)	Maximum conversion efficiency (%)	OLR*	SoA*
[3] (2015)	Four-band 0.9, 1.8, 2.1, 2.4	22	65 at 0 dBm	11	10 × 10
[4] (2016)	Six-band 0.55, 0.75, 0.9, 1.85, 2.15, 2.45	10	67 at -5 dBm	10–75	16 × 16
[5] (2015)	Broad-band 1.8 – 2.5	32.5	70 at 0 dBm	14.7	7 × 7
[7] (2016)	Broad-band 0.47 – 0.99	71	70 at 10 dBm	3, 5.5, 7, 12.2	NA
[8] (2016)	Broad-band 0.6 – 1.15	62.9	80 at 40 dBm	0.034	NA
[13] (2014)	Dual-band 0.915, 2.45	5	70 at 0 dBm	0.5–3	NA
This work without HRCT	Broad-band 0.45 – 0.9	66.7	77 at -1 dBm	5	16 × 16
<b>This work with HRCT</b>	<b>Broad-band 0.47 – 0.88</b>	<b>61</b>	<b>75 at -1 dBm</b>	<b>5–80</b>	16 × 16

\*OLR: Optimal load impedance range with maintained performance (kΩ).

\*SoA: Size of the receiving antenna (cm<sup>2</sup>).

rectenna using the HRCT can maintain the efficiency in a wide load impedance range (from 5 to 80 kΩ), where the efficiency is always higher than 30%. The HRCT can improve the conversion up to 20% when the load resistance is 80 kΩ. In addition, the error bar of the results using the HRCT is smaller than the error bar of the results without using the HRCT. It demonstrates that the non-linear effect of the broadband rectenna has indeed been reduced by the HRCT. A more consistent performance is obtained which is of great importance for wireless energy harvesting used in practice.

A comparison between the rectennas in this paper and some other related rectifiers and rectennas is given in Table II. It can be seen that our rectennas have achieved higher conversion efficiency at lower incident power levels over a very large fractional bandwidth. Moreover, the rectenna design using the proposed HRCT has achieved constant efficiency over the widest load impedance range among others. The proposed HRCT can indeed improve the performance of broadband rectennas.

## V. CONCLUSION

A novel hybrid resistance compression technique has been proposed to improve the performance of broadband rectennas. The HRCT can offer resistance compression and improved impedance matching performance in a wide frequency band. The nonlinear effect of the broadband rectenna can be significantly reduced by using the HRCT. Two ultra-wideband rectennas (with/without using the HRCT) have been made and compared. The measured results have shown that the rectennas have covered the DTV, LTE700, and GSM900 bands (from 0.45 to 0.9 GHz) with a relatively high conversion efficiency (up to 77%). The HRCT can maintain the conversion efficiency

in a wide load impedance range, which is from 5 to 80 kΩ. The measured harvested DC power of the rectennas from an outdoor (open) environment was 66.7 μW. Meanwhile, the proposed rectenna using the HRCT has a consistent conversion efficiency in a wide frequency and load impedance range. Thus it is very suitable for wireless energy harvesting in many real world low power applications, such as wireless sensors, digital clocks, smoke alarms, DC-DC converters, and power management units that normally have different equivalent load impedance.

## REFERENCES

- [1] S. Kim et al, "Ambient RF energy-harvesting technologies for self-sustainable standalone wireless sensor platforms," *Proc. IEEE*, vol. 102, no. 11, pp. 1649–1666, Nov. 2014.
- [2] V. Marian, B. Allard, C. Vollaie, and J. Verdier, "Strategy for microwave energy harvesting from ambient field or a feeding source," *IEEE Trans. Power Electron.*, vol. 27, no. 11, pp. 4481–4491, Nov. 2012.
- [3] V. Kuhn, C. Lahuec, F. Seguin, and C. Person, "A multi-band stacked RF energy harvester with rf-to-dc efficiency up to 84%," *IEEE Trans. Microw. Theory Tech.*, vol. 63, no. 5, pp. 1768–1778, May 2015.
- [4] C. Song, Y. Huang, P. Carter, J. Zhou, S. Yuan, Q. Xu and M. Kod, "A novel six-band dual CP rectenna using improved impedance matching technique for ambient RF energy harvesting," *IEEE Trans. Antennas Propag.*, vol. 64, no. 7, pp. 3160–3171, Jul. 2016.
- [5] C. Song, Y. Huang, J. Zhou, J. Zhang, S. Yuan and P. Carter, "A high-efficiency broadband rectenna for ambient wireless energy harvesting," *IEEE Trans. Antennas Propag.*, vol. 63, no. 8, pp. 3486–3495, May 2015.
- [6] P. Lu, et al., "Polarization reconfigurable broadband rectenna with tunable matching network for microwave power transmission," *IEEE Trans. Antennas Propag.*, vol. 64, no. 3, pp. 1136–1141, Mar. 2016.
- [7] F. Bolos, D. Belo and A. Georgiadis, "A UHF rectifier with one octave bandwidth based on a non-uniform transmission line," *2016 IEEE MTT-S International Microwave Symposium (IMS)*, San Francisco, CA, 2016, pp. 1-3.
- [8] S. Abbasian and T. Johnson, "High efficiency GaN HEMT synchronous rectifier with an octave bandwidth for wireless power applications," *2016 IEEE MTT-S International Microwave Symposium (IMS)*, San Francisco, CA, 2016, pp. 1-4.
- [9] Y. Han, et al., "Resistance compression networks for radio-frequency power conversion," *IEEE Trans. Power Electron.*, vol. 22, no. 1, pp. 41–53, Jan. 2007
- [10] W. Inam, K. K. Afridi, and D. J. Perreault, "High efficiency resonant dc/dc converter utilizing a resistance compression network," *IEEE Trans. Power Electron.*, vol. 29, no. 8, pp. 4126–4135, Aug. 2014.
- [11] T. W. Barton, et al., "Transmission line resistance compression networks and applications to wireless power transfer," *IEEE J. Emerg. Sel. Topics Power Electron.*, vol. 3, no. 1, pp. 252–260, Mar. 2015.
- [12] P. A. Godoy, et al, "Outphasing energy recovery amplifier with resistance compression for improved efficiency," *IEEE Trans. Microw. Theory Techn.*, vol. 57, no. 12, pp. 2895–2906, Dec. 2009
- [13] K. Niotaki, et al., "Dual-band resistance compression networks for improved rectifier performance," *IEEE Trans. Microw. Theory Techn.*, vol. 62, no. 12, pp. 3512–3521, Nov. 2015.
- [14] C. R. Valenta and G. D. Durgin, "Survey of energy-harvester conversion efficiency in far-field, wireless power transfer systems," *IEEE Microw. Mag.*, vol. 15, no. 4, pp. 108–120, May. 2014.
- [15] C. Song, Y. Huang, J. Zhou, P. Carter, S. Yuan, Q. Xu and Z. Fei, "Matching network elimination in broadband rectennas for high-efficiency wireless power transfer and energy harvesting," *IEEE Trans. Ind. Electro.*, vol. PP, no. 99, pp. 1–1, Dec. 2016. DOI: 10.1109/TIE.2016.2645505.
- [16] R. Vyas, B. S. Cook, Y. Kawahara, and M. M. Tentzeris, "E-WEHP: A batteryless embedded sensor-platform wirelessly powered from ambient digital-TV signals," *IEEE Trans. Microw. Theory Techn.*, vol. 61, no.6, pp. 2491–2505, Jun. 2013.